

# Synthesis and Unique Photoluminescence Properties of Nitrogen-Rich Quantum Dots and Their Applications\*\*

Xiuxian Chen, Qingqing Jin, Lizhu Wu, ChenHo Tung, and Xinjing Tang\*

**Abstract:** Nitrogen-rich quantum dots (N-dots) were serendipitously synthesized in methanol or aqueous solution at a reaction temperature as low as 50°C. These N-dots have a small size (less than 10 nm) and contain a high percentage of the element nitrogen, and are thus a new member of quantum-dot family. These N-dots show unique and distinct photoluminescence properties with an increasing percentage of nitrogen compared to the neighboring carbon dots. The photoluminescence behavior was adjusted from blue to green simply through variation of the reaction temperature. Furthermore, the detailed mechanism of N-dot formation was also proposed with the trapped intermediate. These N-dots have also shown promising applications as fluorescent ink and biocompatible staining in *C. elegans*.

Quantum dots, such as gallium arsenide, typically contain a few thousand atoms and have been widely studied since 1990s owing to their useful electronic and photonic properties.<sup>[1]</sup> The small size of these nanostructures results in a quantum confinement of charge carriers (electron–hole pairs).<sup>[2]</sup> This causes a quantization of the energy spectra with discrete energy levels. Based on these specific properties, the applications of these nanostructures have ranged from photonics, electronics, and drug delivery to biological and biomedical imaging in vitro and in vivo.<sup>[3]</sup> However, heavy metals (for example, CdSe, PbTe, and CdTe) as essential elements in semiconductor quantum dots have risks of long-term toxicity and/or potential environmental hazards. Therefore, the needs for more biocompatible nanomaterials with similar properties are urgently required.<sup>[4]</sup> Recently, new quantum dots have been discovered and investigated, such as BN nanosheets, BCNO nanoparticles, nanodiamonds, graphene oxide (GOD), C-dots, and self-assembled nanoparticles.<sup>[5]</sup> Compared to traditional semiconductor quantum dots, carbon based nanostructures<sup>[12]</sup> (such as C-dots, carbon

nanotubes, and GOD) are superior in terms of robust chemical inertness, easy functionalization, high aqueous solubility, low toxicity, and excellent biocompatibility as they do not use heavy metals<sup>[6]</sup> and small hydrophobic molecules.<sup>[7]</sup> They have also attracted great interest in many fields of science owing to their outstanding fundamental properties and show potential exciting applications in many fields,<sup>[13]</sup> such as catalysts,<sup>[8]</sup> bioimaging agents,<sup>[9]</sup> sensors,<sup>[10]</sup> and photovoltaic devices.<sup>[11]</sup> For C-dots, a few percent of nitrogen doping of carbon dots have been reported to give excellent optical properties.<sup>[13c]</sup> However, most of the nitrogen atoms were induced on particle surface under harsh conditions with a few percent of quantum dots by weight, which is much less than the percent of carbon element of the same quantum dots.<sup>[13a,b,14]</sup> Therefore, the desire for new nanostructured materials based on new elements (such as nitrogen) is still challenging.

Fluorescent nitrogen-rich quantum dots (N-dots) were synthesized when 2-azidoimidazole aqueous or methanol solution was inadvertently heated at 70°C overnight without the addition of acids (Figure 1 a). The solution turned dark brown and showed strong cyan-green fluorescence when irradiated with hand-held UV lamp (365 nm). After filtration with a 0.22 µm filter and vacuum-freeze drying, the obtained cinnamon-colored solid residue that was later characterized as nanoparticles was insoluble in common organic solvents (such as ethyl acetate, acetone, chloroform), but was highly dispersible in water. Different from the synthesis of other C-dots under harsh conditions<sup>[15]</sup> (for example: high-energy ion beam radiation, hydrothermal carbonization with extreme high temperature, laser ablation, large amount strong acids), these N-dots were synthesized in a single-step reaction under much milder conditions with 2-azidoimidazole as a starting material. We then expanded the scope of starting materials. However, the raw reaction solution of 3-azidopyrazole, 2,4,6-triazido-1,3,5-triazine, and 3-azido-1,2,4-triazole did not show any photoluminescence and had no nanoparticle formation. The raw reaction solution of 2-azidobenzimidazole showed very weak fluorescence emission with a negligible number of collected nanoparticles (Supporting Information, Figure S1).

UV/Vis absorption and photoluminescence of the N-dot aqueous solution from 2-azidoimidazole were first measured after simple filtration with a 0.22 µm filter. However, their complicated absorption and photoluminescence spectra (Figure 1 b) indicated that the N-dots might have broad size distribution, which is a general disadvantage of bottom-up synthesis strategy for some nanoparticles such as carbon dots.<sup>[16]</sup> To further characterize these N-dots in detail, we turned to separate these N-dots using size-exclusion chromatography with Sephadex G-25, and successfully collected

[\*] X. Chen, Q. Jin, Prof. Dr. X. Tang  
State Key Laboratory of Natural and Biomimetic Drugs  
School of Pharmaceutical Sciences, Peking University  
No. 38, Xueyuan Rd. Beijing 100191 (China)  
E-mail: xinjingt@bjmu.edu.cn  
Prof. L. Wu, Prof. C. Tung  
Technical Institute of Physics and Chemistry  
The Chinese Academy of Sciences (China)

[\*\*] This work was supported by the National Basic Research Program of China (973 Program: 2013CB933800, 2012CB720600), National Natural Science Foundation of China (21372015), and the Innovation Team of the Ministry of Education (BMU20110263). We thank Prof. Ivan Dmochowski for proofreading and helpful suggestions.

Supporting information for this article is available on the WWW under <http://dx.doi.org/10.1002/anie.201408422>.

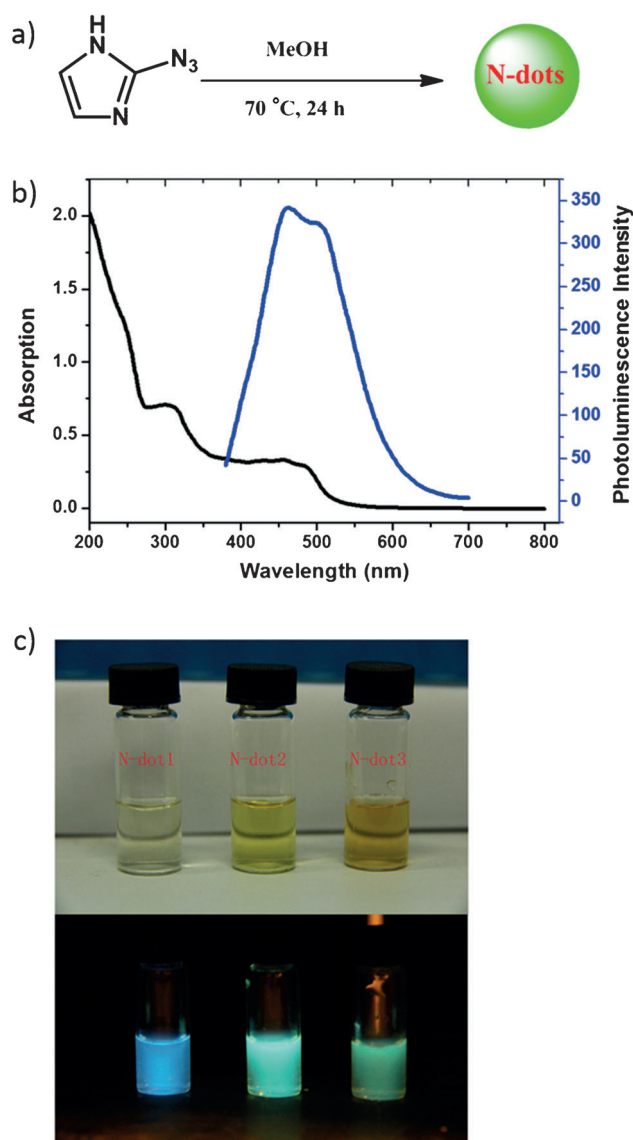


**Figure 1.** a) Synthesis of N-dots. b) UV/Vis absorption spectra of a raw N-dot aqueous solution and photoluminescence emission spectra of a raw N-dot aqueous solution excited at 360 nm. c) Digital image (top) of 0.2 mg mL<sup>-1</sup> N-dots dispersed in pure water and their fluorescent images (bottom) under excitation of hand-held UV lamp (365 nm); from left to right: N-dot 1, N-dot 2, N-dot 3.

three fractions of N-dots according to their elution time. These three kinds of N-dots solutions showed different color and photoluminescence when excited with a hand-held UV lamp (365 nm), named N-dot 1 (blue), N-dot 2 (cyan), and N-dot 3 (cyan green) (Figure 1 c). Further elemental analysis of these N-dots indicated that the nitrogen proportion increased from N-dot 1, N-dot 2, to N-dot 3, in which N-dot 3 had a nitrogen component as high as 34.48 %, about 10 % higher than the carbon content of the same N-dot (Supporting Information, Table S1), which has never been reported previously.<sup>[13c,15a,17]</sup>

Different kinds of microscopy were applied to further verify these N-dots. As shown in Figure 2 a–c, TEM images of N-dot 1, N-dot 2, and N-dot 3 clearly indicated that these N-

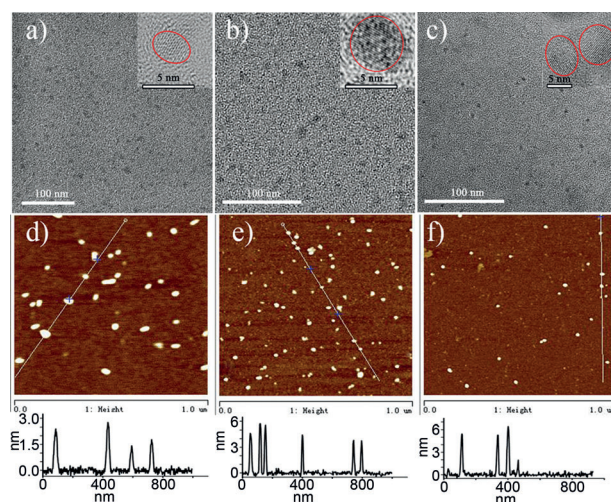


**Figure 2.** a)–c) TEM images of N-dot 1, N-dot 2, N-dot 3 (scale bars 100 nm); Insets are HRTEM images (scale bars 5 nm). d)–f) AFM images and size distributions of N-dot 1, N-dot 2, and N-dot 3. Height profiles are given for the marked white line in the AFM images.

dots are monodisperse nanoparticles with good crystallinity (inserts in Figure 2 a–c). Atomic force microscopy (AFM) was further applied to demonstrate the topographic morphology of N-dots and identify the accurate heights of N-dot 1, N-dot 2, and N-dot 3 (Figure 2 d–f), confirming the homogeneous distribution and height histograms of the N-dots. By quantifying the height of around 70 nanoparticles for each kind of N-dot, the size distributions of these three N-dots (Supporting Information, Figure S2) were  $2.07 \pm 0.61$  nm,  $4.62 \pm 0.64$  nm, and  $5.39 \pm 0.80$  nm in diameter for N-dot 1, N-dot 2, and N-dot 3, which were consistent with their elution times of SEC chromatography. And their sizes were also consistent to the crystal cores of corresponding N-dots (inserts in Figure 2 a–c). Further typical X-ray diffraction (XRD) patterns of all three N-dots show that they had the similar broad peak centered at  $23^\circ$ . The XRD results, along with HRTEM data, illustrated that these N-dots have a crystalline core with an amorphous surface.

We then applied Fourier-transform infrared (FTIR) spectroscopy and X-ray photoelectron spectroscopy (XPS) to further characterize the properties of chemical bonds and functional group on the surface of these N-dots. Figure 3 a demonstrates that N-dot 1, N-dot 2, and N-dot 3 have very similar IR spectra that revealed the existence of functional groups such as OH or NH ( $3415\text{ cm}^{-1}$ ), CH ( $2919\text{ cm}^{-1}$ ,  $2851\text{ cm}^{-1}$ ), C–O–C ( $1082\text{ cm}^{-1}$ ), C=N ( $1545\text{ cm}^{-1}$ ), and C=O ( $1644\text{ cm}^{-1}$ ) on these N-dots.<sup>[13c,18]</sup> In Figure 3 b, the typical XPS surveys of three N-dots indicate a high nitrogen content of these dots, which was consistent to the results of their elemental analysis (Supporting Information, Table S1). The deconvoluted C1s XPS spectrum of N-dot 1 (Supporting Information, Figures S3–S5 and Table S2) indicated four main components assigned as C–C at ca. 284.80 eV, C=N at ca. 286.31 eV, C=O at ca. 287.52 eV, and C–N or C–O at ca. 288.66 eV.<sup>[17]</sup> The N1s XPS spectrum of N-dot 1 around 398.31 eV, 399.23 eV, 399.91 eV and 400.69 eV was pointed to

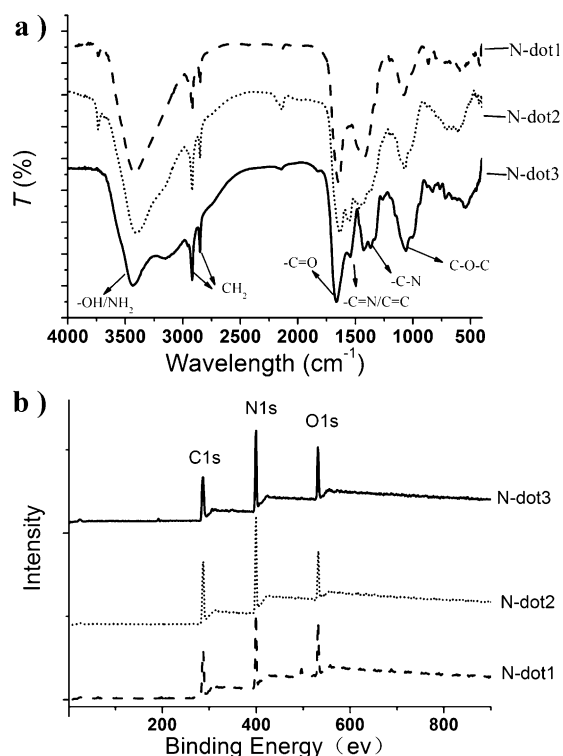


**Figure 3.** a) FTIR spectra and b) XPS survey of N-dot 1, N-dot 2, and N-dot 3.

the nitrogen atom of graphite-like structure, pyridinic-like N and pyrrolic-like N and NH groups, respectively.<sup>[13a,c]</sup> The content of pyrrolic-like N was the most abundant (Supporting Information, Table S3), which indicated a big amount of C=N like groups of N-dots. The O1s XPS spectrum of N-dot 1 could be decomposed into peaks at ca. 530.68 eV, ca. 531.38 eV, ca. 532.24 eV and ca. 532.93 eV, indicating the presence of -OH, \*O=C-O, C-O, and O=C-O\*.<sup>[13c,19]</sup> XPS data of N-dot 2 and N-dot 3 demonstrated that they contained the similar functional groups as N-dot 1 on particle surface (Supporting Information, Table S2). The presence of functional groups<sup>[7b]</sup> (C=N, C-O, NH, OH, etc) imparts excellent solubility in water without the need of further chemical modification of nanoparticle surface. XPS spectra and FTIR spectra, along with element analysis data of N-dots, confirmed that these N-dots contained the elements nitrogen, carbon, oxygen, and hydrogen (Figure 3) with an even higher percentage of nitrogen than carbon both on the surface and in internal crystal core.

The importance of nanoparticle sizes and functional groups for optical properties of N-dots is demonstrated in Figure 4, presenting the optical absorption and photoluminescence spectra of these N-dots. Figure 4a shows that the UV/Vis absorption spectra of N-dot 1 and N-dot 2 have similar absorption curves with an absorption peak around 310 nm, while N-dot 3 had an absorption peak around 310 nm and a broad absorption shoulder peak around 400–500 nm, suggesting a gradual red-shift of their absorption. The photo-

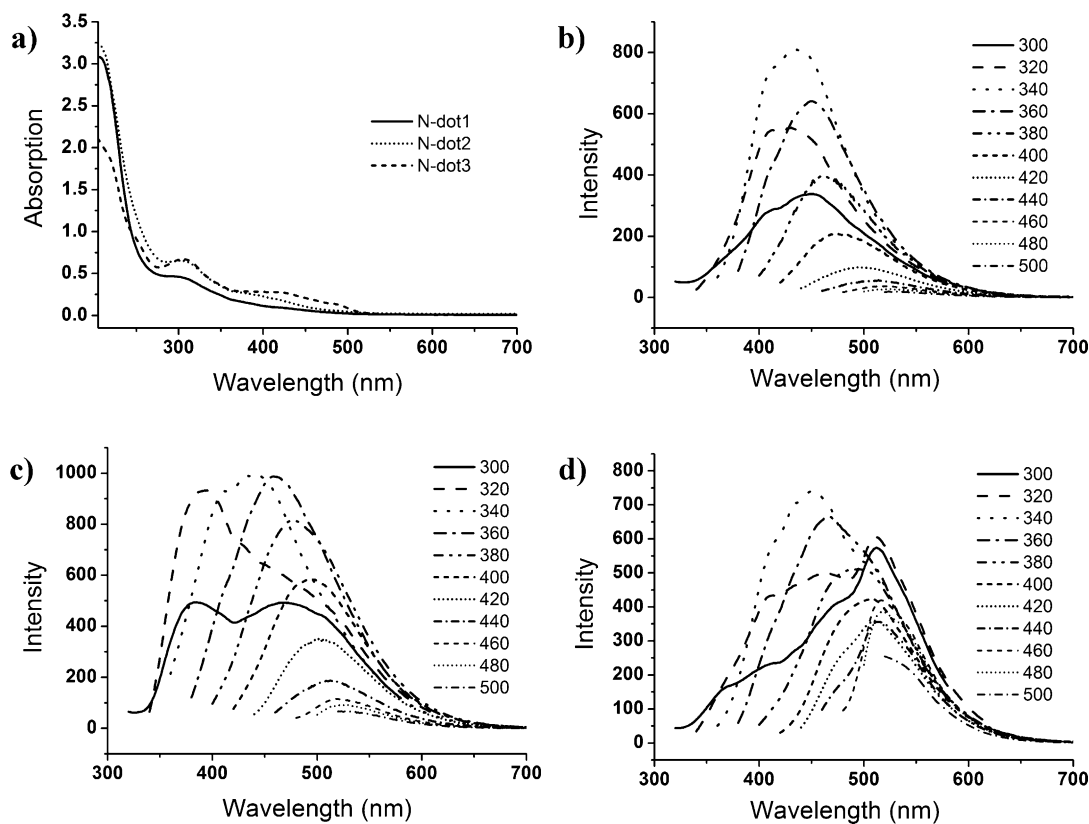
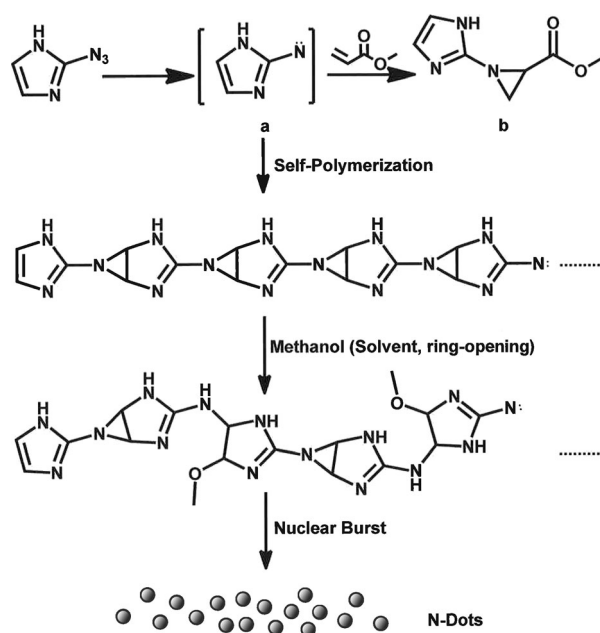


**Figure 4.** a) The UV/Vis absorption spectra of three N-dots (66.7 μg mL<sup>-1</sup>). b)–d) Photoluminescence emission spectra of b) N-dot 1, c) N-dot 2, and d) N-dot 3 recorded from 300 to 500 nm in 20 nm increments.



luminescence spectra of N-dot 1, N-dot 2, and N-dot 3 displayed an emission maximum at 435 nm, 442 nm, and 451 nm, respectively, with the excitation wavelength at 340 nm (Supporting Information, Figure S6), indicating strong quantum confinement of nanoparticles. Figure 4b,c show the red-shift of photoluminescence emission with the reduction of their corresponding intensity as the excitation wavelength increased from 340 to 500 nm in 20 nm increments. Like many C-dots, N-dot 1 and N-dot 2 showed the wavelength-dependent photoluminescence behavior, that is, the observed photoluminescence red-shift of N-dots was accompanied by a significant reduction in photoluminescence intensity that is a signature of the gradual evolution of the confinement in quantum dots. In contrast to N-dot 1 and N-dot 2, N-dot 3 displayed a distinctive photoluminescence performance. Photoluminescence emission of N-dot 3 aqueous solution red-shifted as the excitation wavelength increased between 340 and 400 nm. However, when the excitation wavelength passed over 400 nm, its emission peak centered at 515 nm without obvious decrease in photoluminescence intensity. Interestingly, simply by adjusting the reaction temperature at 50 or 100 °C, we obtained blue photoluminescence and green photoluminescence of the raw N-dot aqueous solutions irradiated by hand-held UV lamp (365 nm) (Supporting Information, Figure S8). N-dots produced at 50 °C showed similar luminescence spectra as N-dot 3 with an emission peak centered at 515 nm, while N-dots produced at 100 °C showed similar luminescence spectra as N-dot 1 with wavelength-dependent photoluminescence behavior (Supporting Information, Figures S9 and S10). Without any surface passivation, the photoluminescence quantum yields of N-dot 1, N-dot 2, and N-dot 3 were 0.10, 0.14 and 0.09, respectively under 360 nm excitation using quinine sulfate in 0.10 M H<sub>2</sub>SO<sub>4</sub> as a reference,<sup>[18b]</sup> which are usually higher than that of C-dots without surface passivation.<sup>[5b,16,20]</sup> According to the photoluminescence mechanism of quantum dots, we expect the photoluminescence quantum yield would be much higher if their surfaces were passivated by polyethylene glycol, metal, etc., as seen for C-dots previously reported.<sup>[5f,6b]</sup>

Although possible mechanisms have been proposed for the formation of carbon dots,<sup>[18b]</sup> no detailed information were provided owing to the harsh synthetic conditions and/or complicated carbonization of carbohydrates. Herein, we proposed a mechanism for the formation of N-dots from 2-azidoimidazole, as shown in Scheme 1. After decomposition of azido moiety, the active intermediate, nitrene, reacted with double bond of 2-azidoimidazole to form tricycle of aziridine moiety and polymers were then formed through self-polymerization. Methanol or water may then be involved in a ring-opening reaction and finally N-dots are formed by probable nuclear burst at supersaturation point.<sup>[18b]</sup> To confirm the mechanism, 2-azidoimidazole was mixed with methyl acrylate at 50 °C for two days. Almost no fluorescence of the reaction solution could be observed; instead, we isolated a new organic compound that proved to be 2-aziridinecarboxylic acid-1-(1H-imidazol-2-yl) methyl ester, a trapped product of active intermediate of self-polymerization. The aziridine moieties in polymers were not very stable and could be attacked by



**Scheme 1.** Proposed mechanism for the formation of N-dots.

solvents (such as methanol and water). The involvement of methanol in N-dots formation was also confirmed by the methoxyl peaks on <sup>1</sup>H NMR and <sup>13</sup>C NMR of N-dots (Supporting Information, Figure S15). The mechanism also explains why no or little N-dots could be formed with other similar starting materials (such as 3-azido-1,2,4-triazole, 3-azidopyrazole, 2,4,6-triazido-1,3,5-triazine). Furthermore, we also found that green photoluminescence of N-dots formed at 50 °C could gradually turn into blue photoluminescence if the 2-azidoimidazole in methanol continued heating at 50 °C for 15 days. This observation could explain the unique photoluminescence properties of N-dot 3 that is possibly due to incomplete ring opening of aziridine moiety by solvents in the formation of N-dots. This is also consistent to the high percentage of nitrogen content in elemental analysis.

The high photoluminescence quantum yields and excitation-wavelength-dependent photoluminescence properties of N-dots make them be a valuable fluorescent ink. The aqueous solutions of N-dots obtained at different reaction temperature (50 °C, 70 °C, 100 °C) were chosen as a new type of fluorescence ink. A calligraphy of letters (N-dots and P, K, U) was then achieved on commercially available filter paper with three N-dot-based fluorescent inks (0.3 mg mL<sup>-1</sup>) using a writing brush. This calligraphy was invisible in daylight, but was clearly observed under a hand-held UV lamp (365 nm, Figure 5a) and remained consistent in an indoor environment, which is beneficial for practical applications. Furthermore, these fluorescent words kept relatively sharp after dipping in water (Supporting Information, Figure S11a), which was not achievable with normal fluorescent ink (fluorescein was used here; Supporting Information, Figure S11b). Not only as fluorescence ink coated on paper, these N-dots could also stain cotton, silk, PAGE gel, and so on (Figure 5; Supporting Information, Figures S12–S14). Figure 5b indicated the cotton was first soaked in N-dots

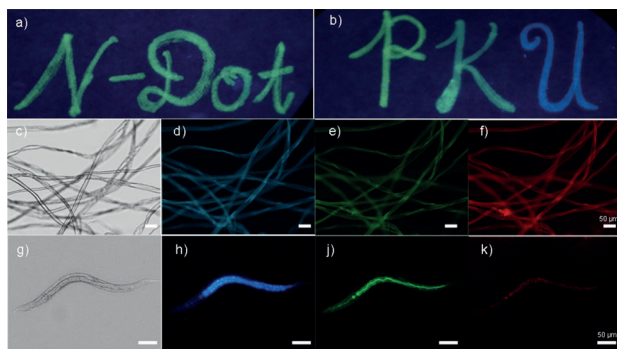


**Figure 5.** a), b) Calligraphy in N-dot-based fluorescent inks with a writing brush on filter paper. “p”, “k”, and “u” were written in different aqueous solutions ( $0.3 \text{ mg mL}^{-1}$ ) of N-dots that were obtained at  $50^\circ\text{C}$ ,  $70^\circ\text{C}$ , and  $100^\circ\text{C}$  respectively, and “N-Dot” was performed in the same ink as “p”. Photos were captured under the excitation of hand-held UV lamp (365 nm). c)–f) Bright-field image and fluorescent images of cotton fibers stained with N-dots ( $0.3 \text{ mg mL}^{-1}$ ). g)–k) Bright-field image and fluorescent images of *C. elegans* stained with an N-dot aqueous solution ( $0.5 \text{ mg mL}^{-1}$ ). Fluorescence images of cotton fibers and *C. elegans* were captured under UV, blue, and green excitation; the fluorescent ink used here was raw N-dot aqueous solution obtained at  $100^\circ\text{C}$ . Scale bars:  $50 \mu\text{m}$ .

aqueous solution ( $0.3 \text{ mg mL}^{-1}$ , N-dots obtained at  $100^\circ\text{C}$ ) for 2 min and then was thoroughly washed. Clear excitation-wavelength-dependent fluorescence was observed under an inverted fluorescence microscope. Under UV, blue, and green light excitation, the cotton fibers showed blue, green, and red fluorescence staining (Figure 5b–e), whereas nearly no fluorescence is observed in the uncoated cotton fibers under the same conditions (Supporting Information, Figure S12). Furthermore, *C. elegans* were also used as a model for N-dot imaging. *C. elegans* were incubated at  $0.5 \text{ mg mL}^{-1}$  raw N-dot solution (N-dots obtained at  $100^\circ\text{C}$ ), and then were imaged under an inverted fluorescence microscope. As shown in Figure 5f–j, cyan, green, and red fluorescence emission were clearly visible under different excitation wavelengths.

In summary, we serendipitously synthesized novel N-dots by using 2-azidoimidazole as a single reactant source under mild conditions, representing a relatively simple and low-cost approach to produce water-soluble quantum dots. A characteristic feature of N-dot synthesis is that neither harsh conditions nor surface passivation is needed. The yield of raw N-dots was about 33%, which was a relatively high yield for the production of quantum dots in comparison to that of carbon dots. By size-exclusive chromatography, we separated three fractions of quantum dots with increasing amount of nitrogen composition by elemental analysis (as high as 34.48%), as confirmed by XPS data. All these quantum dots were then characterized by FTIR, HRTEM, and AFM, and their optical properties were evaluated in detail. The photoluminescence behavior can be adjusted from blue to green simply by the change of reaction temperatures. These results confirmed that these N-dots were indeed nitrogen-rich quantum dots and demonstrated optimal and unique optical properties compared to their neighboring carbon dots, and have shown promising application as fluorescent inks and

biocompatible staining. Furthermore, a detailed mechanism was proposed for the formation of these N-dots through nitrene-mediated self-polymerization and condensation. Future work should be focused on surface modification and their full applications, particularly in biomedical sciences.

Received: August 21, 2014

Published online: October 8, 2014

**Keywords:** bioimaging · fluorescence ink · nanomaterials · photoluminescence · quantum dots

- [1] D. Bera, L. Qian, T.-K. Tseng, P. H. Holloway, *Materials* **2010**, *3*, 2260–2345.
- [2] W. L. Wilson, P. F. Szajowski, L. E. Brus, *Science* **1993**, *262*, 1242–1244.
- [3] a) X. Michalet, F. F. Pinaud, L. A. Bentolila, J. M. Tsay, S. Doose, J. J. Li, G. Sundaresan, A. M. Wu, S. S. Gambhir, S. Weiss, *Science* **2005**, *307*, 538–544; b) C. Wu, D. T. Chiu, *Angew. Chem. Int. Ed.* **2013**, *52*, 3086–3109; *Angew. Chem.* **2013**, *125*, 3164–3190; c) C. X. Guo, H. B. Yang, Z. M. Sheng, Z. S. Lu, Q. L. Song, C. M. Li, *Angew. Chem. Int. Ed.* **2010**, *49*, 3014–3017; *Angew. Chem.* **2010**, *122*, 3078–3081.
- [4] F. Mammeri, A. Ballarin, M. Giraud, G. Brusatin, S. Ammar, *Colloids Surf. A* **2013**, *416*, 1–7.
- [5] a) W. Lei, D. Portehault, R. Dimova, M. Antonietti, *J. Am. Chem. Soc.* **2011**, *133*, 7121–7127; b) D. Pan, L. Guo, J. Zhang, C. Xi, Q. Xue, H. Huang, J. Li, Z. Zhang, W. Yu, Z. Chen, Z. Li, M. Wu, *J. Mater. Chem.* **2012**, *22*, 3314; c) Q. Wu, X. Wang, Q.-S. Li, R.-Q. Zhang, *J. Cluster Sci.* **2013**, *24*, 381–397; d) V. N. Mochalin, O. Shenderova, D. Ho, Y. Gogotsi, *Nat. Nanotechnol.* **2011**, *7*, 11–23; e) L. Shcherbina, T. Torchynska, *Physica E* **2013**, *51*, 65–70; f) Y. Sun, B. Zhou, Y. Lin, W. Wang, K. A. S. Fernando, P. Pathak, M. J. Mezziani, B. A. Harruff, X. Wang, H. Wang, P. G. Luo, H. Yang, E. K. Muhammet, B. Chen, L. M. Vaca, S. Xie, *J. Am. Chem. Soc.* **2006**, *128*, 7756–7757; g) P. Scheiner, *J. Org. Chem.* **1967**, *32*, 2022–2023.
- [6] a) J. Shen, Y. Zhu, X. Yang, C. Li, *Chem. Commun.* **2012**, *48*, 3686–3699; b) P. G. Luo, F. Yang, S.-T. Yang, S. K. Sonkar, L. Yang, J. J. Broglie, Y. Liu, Y.-P. Sun, *RSC Adv.* **2014**, *4*, 10791.
- [7] a) S. Liu, L. Wang, J. Tian, J. Zhai, Y. Luo, W. Lu, X. Sun, *RSC Adv.* **2011**, *1*, 951; b) S. Liu, J. Tian, L. Wang, Y. Luo, X. Sun, *RSC Adv.* **2012**, *2*, 411.
- [8] H. Zhang, H. Ming, S. Lian, H. Huang, H. Li, L. Zhang, Y. Liu, Z. Kang, S.-T. Lee, *Dalton Trans.* **2011**, *40*, 10822.
- [9] a) L. Cao, X. Wang, M. J. Mezziani, F. Lu, F. Wang, P. G. Luo, Y. Lin, B. A. Harruff, L. M. Vaca, D. Murray, S. Xie, Y. Sun, *J. Am. Chem. Soc.* **2007**, *129*, 11318–11319; b) S. Qu, X. Wang, Q. Lu, X. Liu, L. Wang, *Angew. Chem. Int. Ed.* **2012**, *51*, 12215–12218; *Angew. Chem.* **2012**, *124*, 12381–12384; c) S. Zhu, Q. Meng, L. Wang, J. Zhang, Y. Song, H. Jin, K. Zhang, H. Sun, H. Wang, B. Yang, *Angew. Chem. Int. Ed.* **2013**, *52*, 3953–3957; *Angew. Chem.* **2013**, *125*, 4045–4049.
- [10] a) C. Yu, X. Li, F. Zeng, F. Zheng, S. Wu, *Chem. Commun.* **2013**, *49*, 403–405; b) J. M. Liu, L. P. Lin, X. X. Wang, L. Jiao, M. L. Cui, S. L. Jiang, W. L. Cai, L. H. Zhang, Z. Y. Zheng, *Analyst* **2013**, *138*, 278–283.
- [11] S. K. Bhunia, A. Saha, A. R. Maity, S. C. Ray, N. R. Jana, *Sci. Rep.* **2013**, *3*, 1473.
- [12] a) X. Xu, R. Ray, Y. Gu, H. J. Ploehn, L. Gearheart, K. Raker, W. A. Scrivens, *J. Am. Chem. Soc.* **2004**, *126*, 12736–12737; b) H. Li, Z. Kang, Y. Liu, S.-T. Lee, *J. Mater. Chem.* **2012**, *22*, 24230; c) V. Lopez, G. R. Perez, A. Arregui, E. Mateo-Marti, L. Banares, J. A. Martin-Gago, J. M. Soler, J. Gomez-Herrero, F. Zamora, *ACS Nano* **2009**, *3*, 3352–3357.

- [13] a) Y. Xu, M. Wu, Y. Liu, X. Z. Feng, X. B. Yin, X. W. He, Y. K. Zhang, *Chem. Eur. J.* **2013**, *19*, 2276–2283; b) C. Hu, Y. Liu, Y. Yang, J. Cui, Z. Huang, Y. Wang, L. Yang, H. Wang, Y. Xiao, J. Rong, *J. Mater. Chem. B* **2013**, *1*, 39; c) Y.-Q. Zhang, D.-K. Ma, Y. Zhuang, X. Zhang, W. Chen, L.-L. Hong, Q.-X. Yan, K. Yu, S.-M. Huang, *J. Mater. Chem.* **2012**, *22*, 16714.
- [14] Y. Dong, H. Pang, H. B. Yang, C. Guo, J. Shao, Y. Chi, C. M. Li, T. Yu, *Angew. Chem. Int. Ed.* **2013**, *52*, 7800–7804; *Angew. Chem.* **2013**, *125*, 7954–7958.
- [15] a) L. Zhou, B. He, J. Huang, *Chem. Commun.* **2013**, *49*, 8078–8080; b) F. Du, Y. Ming, F. Zeng, C. Yu, S. Wu, *Nanotechnology* **2013**, *24*, 1–9; c) H. Zhu, X. Wang, Y. Li, Z. Wang, F. Yang, X. Yang, *Chem. Commun.* **2009**, 5118–5120.
- [16] Y. Yang, D. Wu, S. Han, P. Hu, R. Liu, *Chem. Commun.* **2013**, *49*, 4920–4922.
- [17] X. Jia, J. Li, E. Wang, *Nanoscale* **2012**, *4*, 5572–5575.
- [18] a) H. Li, X. He, Y. Liu, H. Huang, S. Lian, S.-T. Lee, Z. Kang, *Carbon* **2011**, *49*, 605–609; b) B. De, N. Karak, *RSC Adv.* **2013**, *3*, 8286; c) S. Barman, M. Sadhukhan, *J. Mater. Chem.* **2012**, *22*, 21832–21937.
- [19] S. Sahu, B. Behera, T. K. Maiti, S. Mohapatra, *Chem. Commun.* **2012**, *48*, 8835–8837.
- [20] Q. Liang, W. Ma, Y. Shi, Z. Li, X. Yang, *Carbon* **2013**, *60*, 421–428.